Journal of Reproduction and Development, Vol. 55, No. 1, 2009

—Full Paper—

Second Meiotic Spindle Integrity Requires MEK/MAP Kinase Activity in Mouse Eggs

Mary Ann PETRUNEWICH[1,3], James Robert TRIMARCHI[4]#, Amy Katherine Lindsey HANLAN[1], Mary-Anne HAMMER[1,2] and Jay Martin BALTZ[1–3]

[1]Ottawa Health Research Institute, Ottawa, ON K1Y 4E9, [2]Department of Obstetrics and Gynecology, Division of Reproductive Medicine, [3]Department of Cellular and Molecular Medicine, University of Ottawa, Ottawa, ON K1Y 4E9, Canada and [4]Marine Biological Laboratory, Woods Hole, MA 02543, USA
#Present: Southwestern Vermont Medical Centre, Quality/Safety Department of Bennington, VT 05201, USA

Abstract. ERK-type MAP kinase activity is required for normal first meiotic (MI) metaphase spindle dynamics and first polar body formation at the MI/MII transition, and for MII arrest until egg activation. MEK and MAPK, however, remain active until meiosis is completed and pronuclei form, but whether MEK/MAPK activity affects MII spindle function during egg activation has been unknown. Polarized light microscopy revealed that the MII spindle rapidly (within approximately 15 min) lost birefringence upon treatment of the egg with U0126, indicating decreased organization at the molecular level upon MEK inhibition. In contrast, birefringence rapidly increased when MPF was inhibited with roscovitine, and this was similar to the increased birefringence previously shown after fertilization or parthenogenetic activation with Sr^{2+}. Confocal microscopy indicated that many spindles in U0126-activated eggs had failed to rotate or were dissociated from the egg cortex. Subsequently, abnormally-located midbodies were evident in U0126-induced parthenogenotes. Thus, MEK/MAPK activity is required to maintain the ordered structure of the MII spindle and for normal spindle dynamics during second polar body formation.
Key words: Actin, Cytostatic factor, Meiosis, Mouse, M-phase promoting factor, Parthenogenesis

(**J. Reprod. Dev. 55:** 30–38, 2009)

During meiotic maturation of the oocyte, the spindle undergoes a series of precise movements unique to meiosis. In the mammalian oocyte, the first meiotic metaphase (MI) spindle first forms centrally, then moves parallel to its long axis until it contacts and attaches to the oocyte cortex, permitting highly asymmetric cytokinesis leading to extrusion of the first polar body [1]. The second meiotic metaphase MII spindle then forms and lies parallel to the surface, remaining in this orientation until fertilization [2], when it rotates to once again become perpendicular to the surface, permitting second polar body emission [3–5]. Similar spindle rotations and cortical attachment appear to be a conserved feature of oocyte meiosis, such as in *Xenopus*, *C. elegans*, and *Drosophila* [6–8].

Meiosis is also uniquely characterized by prolonged arrests at specific points in the cell cycle. Active maintenance of MII arrest is controlled by the meiosis-specific cytostatic factor (CSF), which requires constitutive activation of the mitogen-activated protein kinase (MAPK) pathway in the MII oocyte. It is well established that meiotic MAPK activation is controlled by an oocyte-specific protein kinase, MOS, which activates the MAP kinase kinase, MEK, which in turn activates ERK-type MAPKs [9] and downstream effectors that maintain M-phase promoting factor (MPF) activity [10].

Oocytes of *mos*$^{-/-}$ female mice, in which the MOS/MEK/MAPK pathway is inactive, not only fail to arrest in MII, but also produce abnormally large first polar bodies when the MI spindle fails to migrate to the cortex and becomes abnormally elongated before cytokinesis [1, 11–14]. MOS activity is required for normal microtubule organization before and during the MI/MII transition [15]. Direct inhibition of MEK during MI using the specific MEK inhibitor U0126 disrupts the MI spindle and causes formation of abnormally large first polar bodies similar to the *mos*$^{-/-}$ phenotype [16]. In addition, MOS/MEK/MAPK pathway components are physically associated with meiotic spindles, including phosphorylated ERK1/2 MAPK [17, 18], phosphorylated MEK [19, 20] and an ERK1/2 MAPK-interacting protein, DOC1R, whose depletion during MI causes formation of abnormal MII spindles [21]. Thus, it is accepted that MOS/MEK/MAPK activity is required to maintain spindle integrity at the MI/MII transition.

The MOS/MEK/MAPK signaling pathway remains activated, however, until pronuclei are formed several hours after egg activation, thus persisting for a considerable period after CSF activity is no longer required to maintain MII arrest [22, 23]. Since MEK and MAPK are therefore still active during the completion of meiosis, they could also play a role in maintaining MII spindle integrity, rotation and cortical localization during egg activation and formation of the second polar body, analogous to their earlier role at the MI/MII transition. Activated MEK and MAPK both remain associated with MII spindles, and an ERK1/2 MAPK substrate, MISS, is localized specifically to the MII spindle and is required for spindle integrity in mouse oocytes [24], supporting such a role for the MAPK cascade in regulating spindle integrity specifically during MII.

It has not been shown, however, whether MEK/MAPK activity continues to be required to maintain the MII spindle after it has

Accepted for publication: September 6, 2008
Published online in J-STAGE: October 15, 2008
Correspondence: JM Baltz (e-mail: jbaltz@ohri.ca)

formed and is correctly positioned at the cortex. While the *mos*$^{-/-}$ model provides compelling evidence of a requirement for active MEK and MAPK in maintaining the integrity of the spindle at the MI/MII transition, *mos* null oocytes cannot provide evidence that MEK and MAPK have a role in maintaining MII spindle integrity after the MII spindle has formed since the spindle in the *mos*$^{-/-}$ oocyte loses integrity during the MI/MII transition and thus the MII spindle is already abnormal before MII. Therefore, to investigate the role of MEK/MAPK activity specifically during activation of mature eggs with normal MII spindles, we have instead used the highly specific MEK inhibitor U0126, which can quickly inactivate MEK and hence MAPK in MII oocytes [25]. U0126 has been extensively used as a specific MEK inhibitor, including in mammalian MI oocytes, and exposure of maturing MI oocytes to U0126 has been shown to recapitulate the *mos*$^{-/-}$ and MEK knockdown phenotypes at the MI/MII transition [16, 19], validating its use.

Because U0126 inhibits MEK and MAPK activities, and hence inactivates CSF, U0126 treatment parthenogenetically activates MII eggs. We previously found that MII eggs in which MEK was inhibited by U0126 cleaved abnormally and produced a high proportion of activated eggs with large second polar bodies [25], and this provided the motivation for the present study. Although this phenotype was superficially similar to that of *mos*$^{-/-}$ oocytes at the MI/MII transition, the mechanism responsible in MII eggs must be different since, as discussed above, the *mos*$^{-/-}$ phenotype arises from failure of the centrally-located MI spindle to normally migrate to the cortex, while, in contrast, the MII spindle was already located at the cortex in U0126-treated MII eggs. In the present study, we used polarized light and confocal microscopy to determine whether the MII spindle is disrupted when MEK and MAPK are inactivated in MII eggs and to follow the phenotypes of the spindle microtubules and cortical polymerized actin in eggs activated by U0126.

Materials and Methods

Media

The media used for embryo culture were based on KSOM mouse embryo culture medium [26], which contained (in mM) 104 NaCl, 2.5 KCl, 0.35 KH_2PO_4, 0.2 $MgSO_4$, 1 Na lactate, 0.2 glucose, 0.2 Na pyruvate, 25 $NaHCO_3$, 1.7 $CaCl_2$, 1 glutamine, 0.01 tetrasodium EDTA, 0.03 streptomycin SO_4 and 0.16 K penicillin G. Media were supplemented with 1 mg/ml bovine serum albumin (BSA) and equilibrated with 5% CO_2 before use. All media components were purchased from Sigma-Aldrich (St. Louis, MO, USA) and were embryo culture or cell culture grade. For embryo collection and handling, Hepes-KSOM [26] was used and was produced by replacing 21 mM $NaHCO_3$ with equimolar Hepes and adjusting the pH to 7.4 with NaOH. Hepes-KSOM with a reduced Hepes concentration (14 mM) and no BSA was used for embryos during visualization by PolScope [27].

Egg and zygote collection

Female CF1 mice (Charles River Canada, St. Constant, PQ, Canada) were superovulated using 5 IU equine chorionic gonadotropin (eCG; Sigma) followed 48 h later by 5 IU human chorionic gonadotropin (hCG; Sigma). For zygotes, females were caged with BDF males following administration of hCG. Unfertilized eggs were collected 13.5–16 h post-hCG, while zygotes were collected 20–22 h post-hCG. The cumulus was removed by exposure to 300 μg/ml hyaluronidase in Hepes-KSOM for 6–8 min [28]. Eggs were cultured by standard methods [28] in microdrop cultures under mineral oil (Sigma), except where otherwise specified. All procedures involving animals were approved by the Animal Care Committee of the Ottawa Health Research Institute and conformed to the standards of the Canadian Council on Animal Care.

Egg activation

Unfertilized eggs were collected as described above and denuded of cumulus cells by brief exposure to 300 μg/ml hyaluronidase. For parthenogenetic activation with Sr^{2+}, eggs were transferred to 10 mM $SrCl_2$ (Sigma) in Ca^{2+}-free KSOM in microdrops under mineral oil (Sigma) and cultured for 2 h (37 C, 5% CO_2) and then transferred to pre-equilibrated KSOM (37 C, 5%CO_2/air) for timepoints from 2–8 h [29]. For activation with U0126 (Calbiochem, La Jolla, CA, USA), eggs were transferred to 50 μM U0126 in KSOM (37 C, 5% CO_2) and cultured for up to 8 h [25]. We previously showed that the inactive isomer, U0124, had no effect on eggs [25]. For activation with roscovitine (Calbiochem), a modified procedure was used [25]. Because roscovitine appears to be oil-soluble and thus is depleted from culture droplets if they are maintained under oil [30], eggs activated by roscovitine or U0126 and roscovitine simultaneously (U0126+roscovitine, as specified) were cultured in 48-well Nunc culture plates containing 500 μl of media per well. The eggs were washed through one well of KSOM with 50 μM roscovitine (or 50 μM of each roscovitine and U0126, as specified), transferred to a second well containing the same media and then cultured for up to 8 h (37 C, 5%CO_2/air). Stocks of U0126 and roscovitine (50 mM each) were made in DMSO and stored at –20 C.

Kinase assays

MPF and MAP kinase activities were measured simultaneously in lysates of seven pooled eggs or zygotes using histone H1 (Sigma) and Myelin Basic Protein (MBP; Invitrogen Canada, Burlington, ON, Canada) as substrates in an assay modified from that described in Moos *et al*. [31] as previously detailed [25]. This assay has been shown to be specific for the activities of MAPK (as MBP phosphorylation) and MPF (as H1 phosphorylation) in oocytes, if H89(N-[2-((p-bromocinnamyl)amino)ethyl]-5-isoquinolinesulfonamide HCl) is included to inhibit PKA activity and Ca^{2+} is chelated with EGTA (ethylene glycolbis[b-aminoethyl ether]-N,N,N',N'-tetraacetic acid) to inhibit PKC activity [22], as was done here. Briefly, seven eggs or zygotes were blindly selected, pooled, lysed in 3.5 μl kinase lysis buffer [31] and immediately frozen at –80 C. The kinase reaction was initiated at room temperature by the addition of 5 μl of 0.01 mM H89 (Calbiochem), 0.6 mM ATP (Sigma), 2.0 mg/ml histone H1, 1.0 mg/ml MBP and 150 Ci/mmol [γ–^{32}P]ATP (Amersham, Baie d'Urfé, PQ, Canada) in a buffer with 48 mM EGTA as previously described [31]. The reaction was stopped after 30 min by addition of 10 μl 2 × Laemmli sample buffer (Invitrogen) and boiling. The mixtures were separated on 15% SDS-polyacrylamide gels and subsequently dried

[25]. Unfertilized eggs cultured for 8 h and zygotes acted as positive and negative controls, respectively, and the background levels of phosphorylation of MBP and histone H1 were determined from reactions run with lysis buffer only. Quantification was performed by using a Typhoon 8600 with ImageQuant software (Molecular Dynamics, Sunnyvale, CA, USA). Signals were corrected for background by subtracting the intensity in the buffer-only lane. The values of histone H1 or MBP kinase activity for fresh eggs were arbitrarily set at 100%, and other groups were expressed relative to this value within each gel.

Polarized light microscope (PolScope) imaging

A PolScope imaging system (Cambridge Research & Instrumentation, Boston, MA, USA) located at the Marine Biological Laboratory (Woods Hole, MA, USA) was used to measure the birefringence of living eggs and reveal the spindle, as previously described, without the need to fix, stain or label the oocyte [27]. PolScope measures birefringence in the plane of focus independent of orientation and therefore gives also a measure of the degree of coherent organization at the molecular scale in an egg spindle not provided by confocal images. Increased birefringence and hence a more organized spindle was displayed qualitatively on a monochromatic scale from dark gray to white, with white representing the highest birefringence [27].

Eggs were imaged singly using a Zeiss Axiovert 100 inverted microscope equipped with PolScope hardware that was controlled with MetaMorph PolScope software (Universal Imaging Corp., Boston, MA, USA), which was also used for image analysis. Unfertilized eggs were collected and denuded of cumulus cells as described above, except that modified Hepes-KSOM (14 mM Hepes, no BSA) was used during PolScope imaging (above). Eggs were washed in modified Hepes-KSOM and transferred to a plastic tissue culture dish with a cover glass bottom (MatTek Corp., Ashland, MA, USA) using a custom-made heated box for thermal control. For experiments involving U0126 alone, the dish contained 100 μl modified Hepes-KSOM overlaid with mineral oil. When roscovitine was used, the dish contained 900 μl modified Hepes-KSOM and no oil. The dish was allowed to sit in the box for at least 5 min to allow for thermal equilibration prior to the start of image acquisition. A background image was obtained from an area without eggs. Images were acquired periodically during activation experiments at the times indicated. Eggs were imaged prior to activation to establish the baseline spindle appearance. A 6× concentration of the activator (roscovitine, U0126, U0126+roscovitine) was then added to the chamber away from the eggs and was carefully mixed at the time indicated as t=0 for egg activation, in order to yield a final concentration in the chamber of 1×.

Confocal imaging

The protocol for visualizing microtubules was adapted from that of Carabatsos *et al*. [32]. Briefly, eggs were fixed in microtubule stabilization buffer (components from Sigma: 2% formaldehyde, 1 μM paclitaxel, 0.5% Triton and 10 μg/ml aprotinin in Tris-buffered saline [TBS] containing 10 mM Tris-HCl pH 7.5 and 150 mM NaCl) for 30 min at 30 C and then rinsed in blocking solution (2% each of BSA and fetal bovine serum, 0.1 M glycine and 0.01% Triton X-100 in TBS, all components from Sigma). Eggs were then incubated overnight in 20 μg/ml rat anti-tubulin primary antibody (YL1/2, Chemicon, Temecula, CA, USA), incubated for 2–3 h with10 μg/ml Alexa-594 goat anti-rat secondary antibody (Molecular Probes, Eugene, OR, USA), stained for DNA with SyTox Green (1–2 μM; Molecular Probes) and mounted on size 0 coverslips in 75 mg/ml n-propyl gallate (Sigma) in 1:1 glycerol:water (v/v).

For visualizing the distribution of actin filaments (F-actin), eggs were fixed with 2% formaldehyde and 0.02% Triton X-100 in Dulbecco's PBS at 30 C for 30 min, rinsed in blocking solution (above) and incubated overnight (4 C) in TBS with 0.5% Triton, 1% BSA, 5 U/ml Alexa-594-phalloidin (Molecular Probes) and 0.5–1 μM SyTox Green. Eggs were mounted as described for tubulin. The eggs could not be simultaneously imaged for F-actin and tubulin, as the fixation procedure for optimal tubulin visualization was found to significantly inhibit staining of actin filaments with phalloidin in fixed eggs.

Confocal images were collected using an Olympus IX70 inverted microscope equipped with a BioRad MRC-1024 confocal laser-scanning unit and Olympus UApo 40x (NA 1.15) water immersion lens. For Alexa 594 conjugates, excitation was at 594 nm with a helium-neon laser, and the emission image was collected through a 600 nm long pass filter (EFLP). For SyTox Green staining, excitation was at 488 nm with an Argon-ion laser, and the emission image was collected through a band pass filter centered at 522 nm. A series of 9 evenly-spaced confocal sections (approximately 8–10 μm apart) were obtained through the thickness of the egg. The number of eggs analyzed by confocal microscopy in the different treatment groups is specified in the Results.

Data analysis

Graphs were produced using SigmaPlot 8.02 (SPSS, Chicago, IL, USA). For the kinase activity assays, means were tested for significant differences using ANOVA followed by the Tukey-Kramer multiple comparisons post hoc test. Statistical analysis was performed using InStat (GraphPad, San Diego, CA, USA). Polarized light microscopy (PolScope) images are shown in the pseudo-gray-scale provided by the software without adjustment. The overall brightness and contrast of confocal images have been adjusted to optimize visibility of the composite images. In no case did this change the appearance of cellular structures.

Results

MAP kinase and MPF activities during egg activation

Since we used U0126 to inhibit MEK (and hence MAPK) and roscovitine to inhibit the cyclin-dependent kinase (CDK) activity corresponding to MPF, we first confirmed that these inhibitors had the predicted inhibitory effects in MII eggs and determined the time course of inhibition. Histone H1 kinase activity and Myelin Basic Protein (MBP) kinase activity were measured simultaneously in egg lysates as a function of time after egg activation by U0126, roscovitine or U0126+roscovitine added simultaneously (Fig. 1). It has previously been established that the measured H1 kinase activity reflects CDK1 (MPF) activity, while MBP kinase activity reflects ERK-type MAPK activity in oocytes throughout meiosis

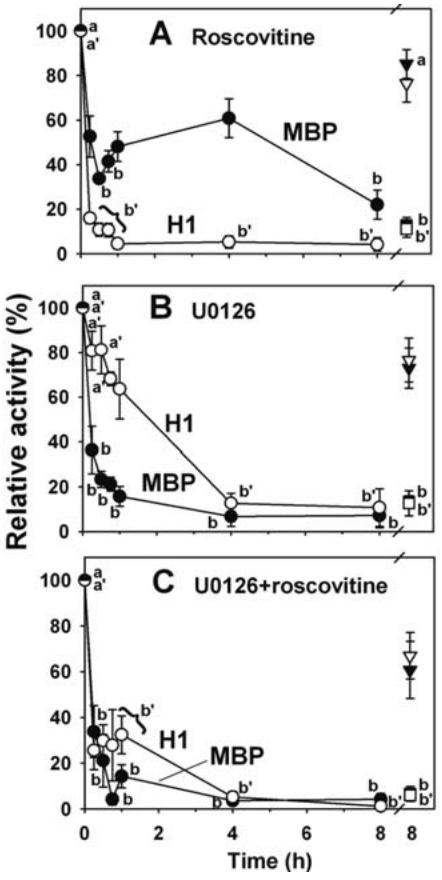

Fig. 1. MAPK and MPF activities as a function of time after egg activation. MBP kinase (MAPK; closed symbols) and Histone H1 kinase (MPF; open symbols) activities were measured simultaneously in each sample of MII eggs (circles) activated with roscovitine (A), U0126 (B) or U0126+roscovitine (C). Activities are expressed relative to the activity in unactivated MII eggs (t=0) included on the same gel, which was arbitrarily set to 100%. As controls, each gel also included pronuclear stage 1-cell embryos (squares) and unfertilized eggs (inverted triangles) that were maintained in culture for 8 h before measurement. Each point is the mean ± SEM of N=7–8 replicates for t=0, t=1 h, 1c and unfertilized eggs, 4–5 replicates for 4 h and 8 h and 3–4 replicates for the remaining time points. ANOVA followed by Tukey-Kramer post hoc test was used to determine points that were significantly different ($P<0.05$) from unactivated eggs at t=0 and from pronuclear stage 1-cell embryos. All points that are not significantly different from the kinase activities in unactivated eggs at t=0 are marked "a" for MBP kinase (MAPK) activity and "a′" for Histone H1 kinase (MPF) activity. Similarly, points not significantly different from the kinase activities in pronuclear stage 1-cell embryos (after both MAPK and MPF were inactivated) are marked with "b" for MBP kinase and "b′" for Histone H1 kinase.

[22].

When eggs were exposed to roscovitine (Fig. 1A), H1 kinase (MPF) activity fell within 15 min to less than 20% of its value in unfertilized eggs and was undetectable above the background by 1 h. In the same eggs, MBP kinase (MAPK) activity remained elevated for at least 4 h, but decreased to baseline by 8 h. This is similar to the timecourses for each kinase activity previously determined in eggs after *in vitro* fertilization [25] and in parthenogenotes after Sr^{2+}-activation [29]. In contrast, eggs treated with U0126 (Fig. 1B) exhibited a rapid loss of MBP kinase (MAPK) activity, which dropped to <40% within 15 min and to background within 1 h, while H1 kinase (MPF) activity decreased more slowly and remained high (approximately 60% of initial activity) at 1 h. When both inhibitors were used simultaneously to activate eggs (Fig. 1C), both kinase activities decreased rapidly and with similar timecourses to those seen when each inhibitor was used individually.

As described below, the critical period for the onset of abnormal spindle and egg morphology was within approximately the first hour, with effects on the spindle organization as detected by PolScope evident within 20 min. During this period, the three treatments generated three different patterns of the two kinase activities. Roscovitine-activated eggs had elevated MAPK and low MPF activities, which is similar to Sr^{2+}-activated or fertilized eggs [29]. U0126-activated eggs had the opposite pattern, with high MPF and low MAPK. Finally, U0126 and roscovitine together (U0126+roscovitine) produced activated eggs with low levels of both activities during this period.

Spindle dynamics and organization in living eggs following egg activation

Polarized light microscopy directly reveals the amount of ordered structure in the spindle as birefringence [5], which provides a measure of periodic, anisotropic structure at the scale of the wavelength of light (e.g., aligned spindle microtubules). When eggs were activated with roscovitine alone, the birefringence of almost all spindles increased markedly (Table 1; Fig 2A). The initial increase in birefringence was observed in images starting at 8–15 min after introduction of roscovitine and reached a maximum after about 15–35 min (Fig. 2A). This closely resembled the increase in spindle birefringence previously shown to be one of the earliest manifestations of egg activation with Ca^{2+} ionophore [5] or with Sr^{2+} [33] and confirmed that eggs in which MPF is inactivated but whose MEK/MAPK activity remains high show increased order in the spindle, even in the absence of increased intracellular Ca^{2+}. All roscovitine-activated eggs that were examined extruded the second polar body at times raging from 35–60 min after roscovitine addition, and at this time the birefringence of the spindle increased further when the midbody was formed between egg and polar body. This result indicates that the increase in spindle order that normally occurs at egg activation is the result of decreased MPF activity and that it is independent of Ca^{2+}.

In contrast, in eggs activated with U0126, increased birefringence was not observed in any egg (Table 1). Instead, there was either no change during the first hour after U0126 was introduced or the spindle dimmed and became undetectable by PolScope, indicating that its birefringence had decreased to the point where it was not greater than that of the essentially isotropic cytoplasm. In the cases where spindle birefringence became undetectable (Fig. 2B), this occurred within 12–18 min post-U0126, i.e., at approximately the time post-activation that increased birefringence was normally

Table 1. Changes in spindle birefringence after MII egg activation

Birefringence	U0126	Roscovitine	U0126+roscovitine
Increased	0 (0%)	9 (90%) [a]	0 (0%)
Decreased [b]	6 (55%)	0 (0%)	9 (100%)
Unchanged	5 (45%)	1 (10%)	0 (0%)
Total (N)	11	10	9

[a] Data are presented as the number of eggs (% of total). Each egg constituted a separate experiment, as one activated egg was imaged in each experiment. [b] In eggs scored as decreased, the spindle became undetectable by polarized light microscopy (i.e., birefringence was not detectably different from cytoplasm). There is a significant association between rows and columns (P<0.0001 by chi-square test).

expected. Disappearance of spindle birefringence in images was not due to the spindle having moved out of focus, since dimming of birefringence was observable in sequential images and focusing through the egg after spindle disappearance failed to reveal a birefringent spindle (not shown). Similarly, in eggs treated with U0126+roscovitine, birefringence decreased and the spindle became undetectable in all eggs by 8–20 min after the inhibitors were introduced (Table 1 and Fig. 2C). This indicated that the apparent decrease in ordered structure in the spindle that occurred when MEK/MAPK were inhibited by U0126 was dominant over the increase in birefringence normally seen with roscovitine. Thus, unlike eggs activated by fertilization or Sr^{2+} (previous results) or by inhibition of MPF activity with roscovitine, in which the ordered anisotropic structure of the spindle increases, inhibition of MEK with U0126 produced a clear loss of organization in the spindles of MII eggs even though they became activated.

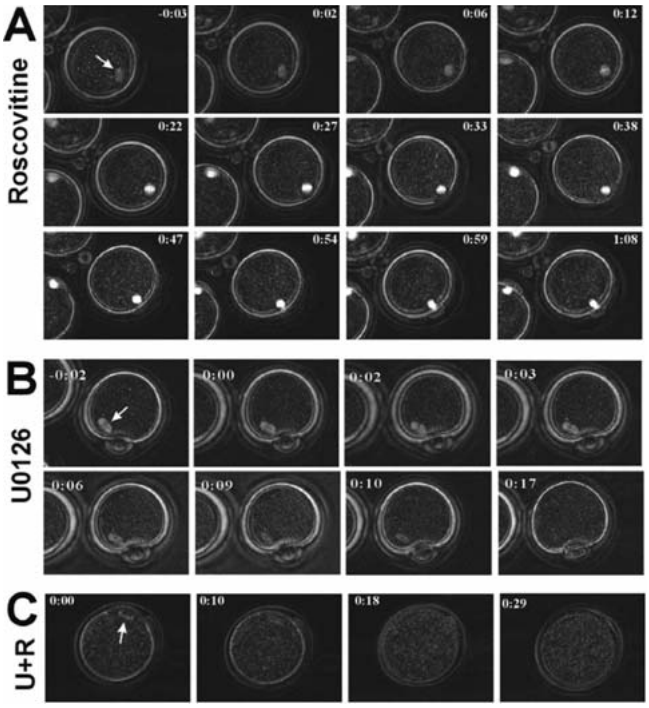

Fig. 2. Rapid loss of ordered structure in the metaphase II spindle upon MEK inhibition as revealed by birefringence measurements using polarizing light microscopy (PolScope). Eggs were activated with roscovitine (A), U0126 (B) and U0126+roscovitine (C) while images were acquired. Within each panel (A, B or C), sequential images represent a time series of images of a single egg during activation. The numbers at the top of each image are the time, in hours:minutes, relative to egg activation by addition of the specified inhibitor to the bath at t=0. Spindle positions are indicated by the arrow in the first image of each series. With roscovitine (A), the spindle increased in brightness, indicating increased birefringence (compare images at 0:06,0:12, and 0:22), while in both groups with U0126 (B, C), the spindle dimmed and eventually was not visible in polarized light. In the roscovitine-activated egg, spindle rotation and formation of the second polar body are evident. The eggs are approximately 75 μm in diameter.

Spindle characteristics after egg activation

To determine whether the apparent rapid destabilization of the spindle structure by U0126 treatment as indicated by polarized light microscopy had consequences for subsequent spindle localization, we used confocal microscopy with immunostaining for tubulin to examine the position and morphology of spindles after U0126 treatment. We first confirmed that unfertilized MII eggs showed the expected spindle morphology. Confocal microscopy of tubulin in MII-arrested unfertilized eggs (N=43) showed that the MII spindle was located immediately under the cortex, with its long axis parallel to the egg surface in the large majority (N=39/43) of MII eggs (not shown). Of the remaining eggs, one appeared to have become spontaneously activated and entered anaphase, while the other three had disrupted spindles. Thus, approximately 10% of eggs used here had apparently abnormal spindles before activation, and this indicates the possible proportion of abnormal spindles due to abnormalities already present in the MII egg.

We assessed spindle morphology during the initial stages of egg activation with U0126, roscovitine, U0126+roscovitine or Sr^{2+} using confocal microscopy with immunocytochemistry for tubulin. Although only single sections are shown in the examples, entire sets of nine sections were used to determine the three-dimensional position of the spindle when categorizing the phenotype. Examining eggs fixed at 1–3 h after these treatments showed that the transition from metaphase to anaphase occurred more slowly in eggs treated with U0126, roscovitine or U0126+roscovitine than in eggs activated with Sr^{2+}. Spindle rotation and transition to anaphase was complete in all Sr^{2+}-activated eggs examined by 1 h, but the majority of eggs treated with roscovitine, U0126 or

Table 2. Spindle phenotype in eggs 3 h after treatment

Treatment	N	Metaphase spindle		Activated					
				Rotated [b]		Normal midbody		Abnormal drifted, parallel [c]	
U0126	38	5	(13)[a]	1	(3)	9	(24)	23	(60)
Roscovitine	9	0	(0)	1	(11)	7	(78)	1	(11)
U0126+roscovitine	16	0	(0)	2	(12)	6	(38)	8	(50)
Sr^{2+}	8	0	(0)	0	(0)	8	(100)	0	(0)

[a] Number of eggs (%). [b] Rotated included mainly anaphase/telophase spindles that had rotated out of parallel. [c] The status of the spindle or remnant in 1 egg in each of the roscovitine and U0126+roscovitine groups was unclear. These are included in the abnormal category.

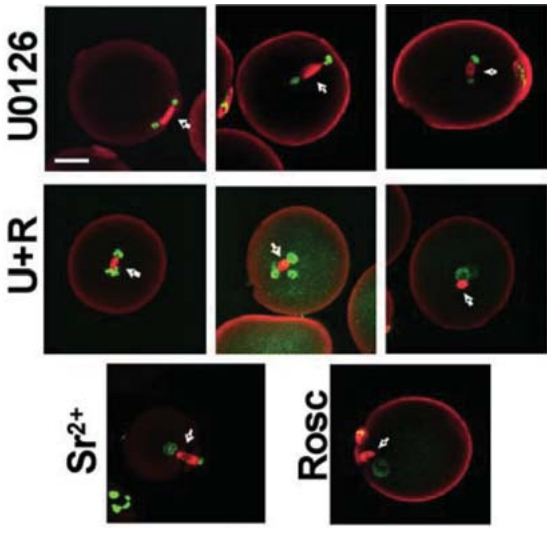

Fig. 3. Examples of spindle phenotypes after egg activation by U0126. Three examples each of an egg after activation with U0126 (top row) or U0126+roscovitine (U+R; second row) are shown (3 h post-activation). Many U0126-activated eggs (top) exhibited spindles that had failed to rotate (left) or had drifted away from the cortex (middle, right). Similarly, those activated by U0126+roscovitine simultaneously had a large number of spindles that were far from the cortex (all 3 examples). Examples of normal polar bodies with midbodies resulting from egg activation with Sr^{2+} or roscovitine (rosc) are shown at the bottom. DNA is shown in green, and tubulin is shown in red. The spindle or spindle remnant is indicated with arrows. The scale bar at the top left is approximately 20 μm and applies to all sections in the figure.

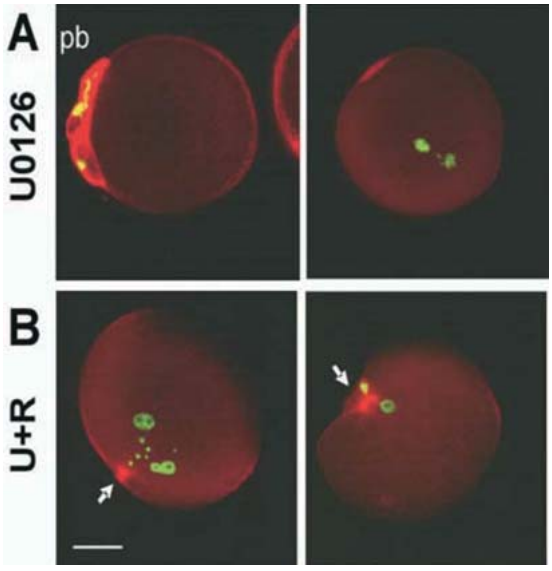

Fig. 4. Examples of the actin distribution after egg activation by U0126. Actin was distributed mainly in the polar bodies ("pb") of eggs that emitted them after activation with U0126 (A; 3 h post-activation). In U0126-activated eggs, the spindles of which had apparently drifted away from the cortex before anaphase (top right), less actin was evident (the patch of staining may be the remnant of the first polar body). In contrast, eggs activated with U0126+roscovitine simultaneously (B) showed predominantly foci of actin (arrow) at the cortex near the location of the DNA. DNA is shown in green, and actin is shown in red. The scale bar at the bottom left is approximately 20 μm and applies to all sections in the figure.

U0126+roscovitine did not undergo these transitions until about 2 h after treatment (not shown). Therefore, we assessed spindle morphology at 3 h, when nearly all (80–100%) eggs in each group had exited metaphase.

A majority of eggs that had been activated with U0126 showed abnormal remnants of spindles at 3 h (Table 2). Only a minority of those eggs assessed had a normal midbody located between the egg and a small polar body, while the largest proportion (approximately 60%) showed spindle remnants that had apparently drifted away from the egg cortex and were localized deeper in the cytoplasm, or were activated but still parallel to the egg cortex (Fig. 3). This was essentially unchanged when eggs were also exposed to roscovitine simultaneously with U0126 (U+R). In contrast, eggs exposed to roscovitine alone mainly showed a normal midbody, and this was similar to eggs activated by Sr^{2+} (Table 2, Fig. 3). The main effect of the presence of U0126, therefore, was a tendency for the spindle to be in an abnormal position in the egg by several hours after exposure.

We also attempted to test whether U0126 perturbed activation by Sr^{2+}, since Sr^{2+} induces a transient increase in intracellular Ca^{2+} and morphologically normal parthenogenotes similar to those that result from fertilization. However, we found that few eggs sur-

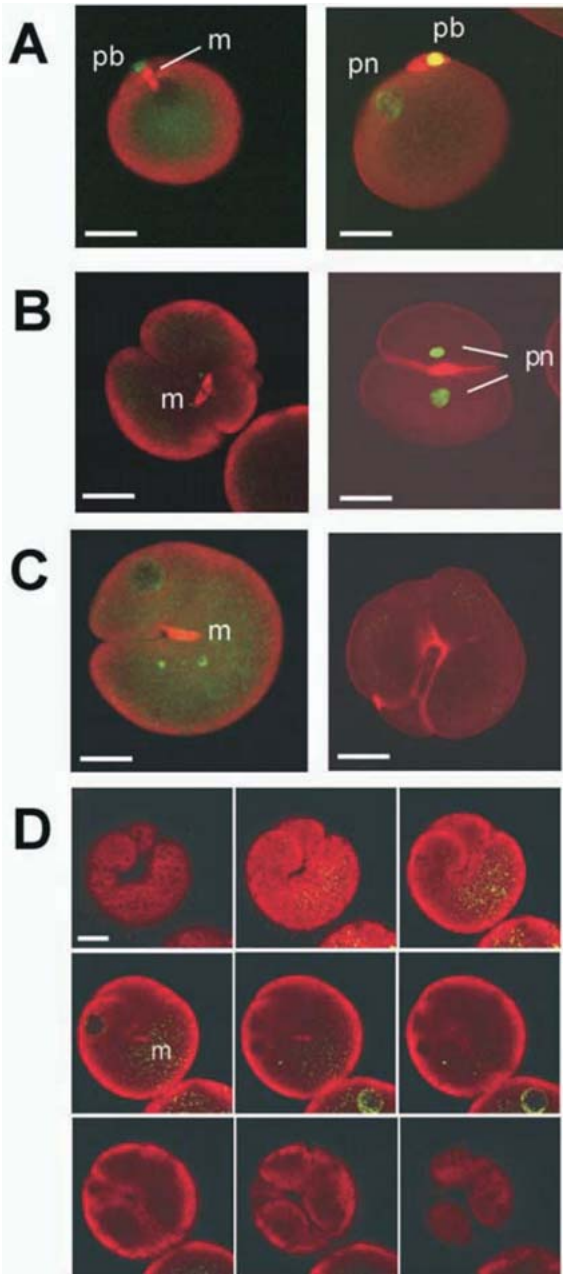

Fig. 5. Examples of the tubulin and actin distributions in parthenogenotes after activation with U0126. This figure shows individual, representative examples of parthenogenotes at 7–8 h after activation with U0126 or U0126+roscovitine. The structures are labeled as follows: midbody (m), polar body (pb) and pronucleus (pn). A) The tubulin (left) and actin (right) distributions in U0126-activated parthenogenotes with a phenotype resembling normal activated eggs with a small 2nd polar body. The midbody is visible between the polar body and egg (left). A pronucleus can be seen in the confocal section on the right, but the pronucleus was not included in the section on the left. B) The tubulin (left) and actin (right) distributions in U0126-activated parthenogenotes with a very large 2nd polar body. A midbody is visible at the juncture of the egg and a large polar body (which may have cleaved). Two pronuclei, one in the activated egg and one in the large polar body, are visible in the section on the right. C) Examples of the multi-lobed phenotype that arose when eggs were activated with U0126+roscovitine simultaneously. Staining for tubulin revealed midbody-like structures visible near the centre of the egg (left). The localization of the midbody near the focus of invaginations is apparent. When similar parthenogenotes were stained for actin (right), a bright focus of actin was visible at the sites of invaginations, with most connected to networks of actin extending around the cortex of the cells where lobes had developed. D) A complete series of nine confocal sections of a single parthenogenote stained for tubulin after activation with U0126+roscovitine clearly shows the typical lobular structure with incomplete cleavage. A midbody is visible in the 4th and 5th sections (marked in the 5th section) lying at the bottoms of invaginations from both above and below. DNA is shown in green, and tubulin (A–C left, D) or actin (A–C right) is shown in red. Scale bars indicate approximately 20 μm.

vived co-treatment with Sr^{2+} and U0126 and so were unable to perform such experiments (3 separate repeats, not shown).

Actin morphology after egg activation

In normal egg activation, an actin-rich cortical patch that overlies the MII spindle disappears in most eggs within approximately 1 h post-activation, and this is followed by cytokinesis of the second polar body which then contains most of the brightly-stained F-actin. By 3 h post-activation, which is when the spindles were assessed (above), bright actin staining is mainly found in the polar body, which we confirmed here (not shown). Eggs activated by roscovitine also mainly (N=14/18) exhibited this normal pattern (not shown).

Many eggs activated with U0126 also exhibited a similar pattern of F-actin, although a substantial number of the remainder lacked visible actin staining. At 3 h, approximately 80% (N=14/18) of the eggs assessed had brightly-stained second polar bodies, while the remainder had chromosomes that had drifted away from the cortex and had little actin staining (Fig. 4A). Thus, activated eggs which formed second polar bodies exhibited actin staining mainly in the polar bodies, while a cohort in the U0126-activated group in which the chromosomes were visible away from the cortex did not possess second polar bodies and had little visible actin staining (except in first polar bodies or remnants).

A different pattern of actin distribution was seen after egg activation with U0126+roscovitine. At 3 h, only approximately 10% (N=3/34) had produced normal-appearing polar bodies. The majority (approximately 65%) had condensed foci of actin (Fig. 4B), either as bright, concentrated areas of staining (N=18/34) or as more diffuse networks of actin staining (N=4/34). The remainder either still retained actin-rich patches (N=5/34) or had little or no visible actin staining (N=3/34). Thus, the majority of eggs activated by U0126 and roscovitine simultaneously had actin foci, while this was not seen in eggs activated by Sr^{2+}, roscovitine or U0126 alone.

Actin and tubulin distributions in pronuclear stage parthenogenotes

We also examined the further development of parthenogenotes produced by activation with U0126. U0126-activated eggs that possessed an apparently normal-sized second polar body (N=10 each h from 4–8 h) mainly (60–70%) showed a normal midbody and actin staining in the polar body (Fig. 5A), and this was similar to the actin and tubulin distributions in Sr^{2+} or roscovitine-activated eggs 4–8 h after activation (not shown).

A number of U0126-activated eggs examined from 4–8 h post-activation had abnormally large second polar bodies (Fig. 5B) as previously reported [25]. These eggs also mainly possessed midbodies localized between the cleaved cells (N=14/21), and they exhibited actin staining mainly in the cleavage plane.

The majority of U0126+roscovitine-activated parthenogenotes 4–8 h after activation were of the distorted phenotype previously reported [25]. When stained for tubulin, these parthenogenotes mainly exhibited structures resembling midbodies (85%, N=28/33; the remainder had no tubulin staining), which were usually found deep in the cytoplasm, often at the site of invaginations that produced the characteristic lobular phenotypes of these eggs (Fig. 5C and D). Actin mainly appeared as a bright focus or a network of filaments. At 4–5 h post-activation, most eggs still only had a single focus of actin (30%, N=9/30 at 4 h; 35%, N=9/26 at 5 h) or a network of actin on the surface, usually with a bright focus from which it radiated (37%, N=11/30 at 4 h; 50%, N=13/26 at 5 h). From 6 h onwards, eggs mainly exhibited extensive networks of actin (Fig. 5C, right), usually following the contours of the distorted eggs.

Discussion

We previously found that U0126, a specific inhibitor of activated MEK [34], but not its inactive analog U0124, was sufficient to parthenogenetically activate MII mouse eggs and that it frequently produced a characteristic phenotype with large polar bodies or nearly symmetric cleavages [25]. In the present study, we have shown that inhibition of MEK and MAPK inactivation with U0126 in MII eggs caused an evident destabilization of the MII spindle that occurred rapidly after MEK inhibition, apparently leading to the development of these abnormal phenotypes.

Polarized light microscopy (PolScope imaging) revealed that there was an unexpectedly rapid decrease in the birefringence of most MII spindles following introduction of U0126, which usually resulted in spindles becoming undetectable by polarized light microscopy within approximately 10–20 min. The decreased birefringence indicates substantial loss of ordered, anisotropic structure in the spindle. This apparent loss of organized spindle structure occurred over the same period during which we found that MEK/MAPK inactivation occurred. In contrast, egg activation using roscovitine (in the present study), Ca^{2+} ionophore [5] or Sr^{2+} [33] instead caused a very marked increase in spindle birefringence, indicating that spindle structure normally becomes much more ordered and exhibits markedly increased anisotropy shortly after egg activation. We interpret this to indicate that MEK/MAPK activity is required to maintain the structural integrity of the MII spindle, rather than being a secondary effect of U0126-induced release from MII arrest, since the loss of structure revealed by polarized light microscopy occurred before MPF activity began to decrease (initiating release from arrest). Our results are thus consistent with a model in which MII spindle integrity requires MEK and MAPK activity both before and during egg activation, and where, in the absence of active MEK/MAPK, the MII spindle loses structural integrity and the normal increase in ordered spindle structure during egg activation fails to occur. In contrast, during normal fertilization (or in eggs activated by Sr^{2+} or roscovitine), the decrease in MPF while MEK/MAPK activity is maintained instead causes a marked increase in ordered structure in the spindle.

Confocal microscopy showed that, following egg activation with U0126, many spindles had either drifted away from the cortex or failed to rotate normally and were still parallel to it. This contrasts with eggs activated using Sr^{2+}; these eggs had spindles that always entered anaphase only while attached to the cortex and after they had rotated to become perpendicular to the cortex, following which they completed a highly asymmetric cytokinesis to produce normal small second polar bodies. At later time points, midbodies in U0126-activated eggs were often found at the cleavage plain with abnormally large polar bodies, implying that cleavage was induced through the spindle after it had drifted away from the cortex or while it was abnormally oriented. Thus, we propose that the large second polar body phenotype that often arises when MEK is inhibited in MII eggs is due to loss of cortical attachment of the MII spindle, so that the spindle drifts into the cytoplasm and induces a cleavage plane deeper in the egg than normal, or is due to incomplete rotation of the spindle, either of which induces cleavage planes more nearly perpendicular to the egg surface than normal. In either case, the consequent cleavage plain induced at cytokinesis passes deeper through the egg than in fertilized eggs, and this results in a polar body that is abnormally large. This contrasts with the etiology of the large first polar body phenotype in *mos*$^{-/-}$ oocytes, which is instead the result of failure of the MI spindle to move to the cortex and subsequent spindle stretching [1, 14].

Eggs activated by U0126+roscovitine simultaneously almost never formed polar bodies but instead first produced a focus of actin on the cortex and subsequently produced a multilobed phenotype with a spindle remnant at the site of deepest invagination, which was not observed with any other means of egg activation. We hypothesize that this difference may be due to the timing of MPF inactivation with respect to spindle destabilization by MEK inactivation with U0126. With U0126 alone, the disrupted spindle usually lost its normal cortical localization before MPF inactivation, exit from MII and initiation of anaphase. In contrast, with U0126+roscovitine, spindle disruption and MPF inactivation occurred nearly simultaneously so that the spindle was still localized at the cortex during the initiation of egg activation. Actin organization by chromatin is dependent on the distance between egg chromosomes and the cortex [35, 36]. We therefore hypothesize that a spindle localized at the cortex is able to strongly induce actin polymerization, but because the spindle is disorganized, the result is not a normal symmetric ring but only a condensation of actin into a single focus that then contracts to form the observed lobes. Since the focus of condensed actin was found nearest the spindle, this would also explain the observation of a midbody-like

structure under the deepest invaginations at later time points.

In summary, the results presented here indicate that MEK and MAPK activity continue to be required for maintaining spindle integrity in the mature MII egg at activation, and this is similar to their well-established role at the MI/MII transition. The normal increase in ordered MII spindle structure upon egg activation is due to decreased MPF activity and is apparently independent of the fertilization-induced Ca^{2+} transient. In the absence of MEK and MAPK activity, the MII spindle fails to exhibit increased order during egg activation and instead often shows a marked decrease in ordered structure in the spindle. The spindle then frequently loses its cortical localization or fails to rotate normally, leading to a high incidence of abnormal cleavage patterns during second polar body emission.

Acknowledgements

The authors would like to thank Dr. D Albertini for his generous help and advice, Dr. A Risdale for expert assistance with confocal microscopy and Ms. K Courville for excellent technical support. This work was supported by Canadian Institutes of Health Research Operating Grant MOP74515 to JMB. MAP was partially supported by an Ontario Graduate Scholarship and a Government of Ontario-Loeb Health Research Institute Graduate Scholarship in Science and Technology.

References

1. **Verlhac MH, Lefebvre C, Guillaud P, Rassinier P, Maro B**. Asymmetric division in mouse oocytes: with or without Mos. *Curr Biol* 2000; 10: 1303–1306.
2. **Kubiak JZ, Weber M, Geraud G, Maro B**. Cell cycle modification during the transitions between meiotic M-phases in mouse oocytes. *J Cell Sci* 1992; 102 (Pt 3): 457–467.
3. **Maro B, Johnson MH, Pickering SJ, Flach G**. Changes in actin distribution during fertilization of the mouse egg. *J Embryol Exp Morphol* 1984; 81: 211–237.
4. **Zhu ZY, Chen DY, Li JS, Lian L, Lei L, Han ZM, Sun QY**. Rotation of meiotic spindle is controlled by microfilaments in mouse oocytes. *Biol Reprod* 2003; 68: 943–946.
5. **Liu L, Trimarchi JR, Oldenbourg R, Keefe DL**. Increased birefringence in the meiotic spindle provides a new marker for the onset of activation in living oocytes. *Biol Reprod* 2000; 63: 251–258.
6. **Gard DL**. Microtubule organization during maturation of Xenopus oocytes: assembly and rotation of the meiotic spindles. *Dev Biol* 1992; 151: 516–530.
7. **Endow SA, Komma DJ**. Spindle dynamics during meiosis in Drosophila oocytes. *J Cell Biol* 1997; 137: 1321–1336.
8. **Yang HY, McNally K, McNally FJ**. MEI-1/katanin is required for translocation of the meiosis I spindle to the oocyte cortex in C elegans. *Dev Biol* 2003; 260: 245–259.
9. **Fan HY, Sun QY**. Involvement of mitogen-activated protein kinase cascade during oocyte maturation and fertilization in mammals. *Biol Reprod* 2004; 70: 535–547.
10. **Madgwick S, Jones KT**. How eggs arrest at metaphase II: MPF stabilisation plus APC/C inhibition equals cytostatic factor. *Cell Div* 2007; 2: 4.
11. **Hirao Y, Eppig JJ**. Parthenogenetic development of Mos-deficient mouse oocytes. *Mol Reprod Dev* 1997; 48: 391–396.
12. **Colledge WH, Carlton MB, Udy GB, Evans MJ**. Disruption of c-mos causes parthenogenetic development of unfertilized mouse eggs. *Nature* 1994; 370: 65–68.
13. **Hashimoto N, Watanabe N, Furuta Y, Tamemoto H, Sagata N, Yokoyama M, Okazaki K, Nagayoshi M, Takeda N, Ikawa Y**. Parthenogenetic activation of oocytes in c-mos-deficient mice. *Nature* 1994; 370: 68–71.
14. **Choi T, Fukasawa K, Zhou R, Tessarollo L, Borror K, Resau J, Vande Woude GF**. The Mos/mitogen-activated protein kinase (MAPK) pathway regulates the size and degradation of the first polar body in maturing mouse oocytes. *PNAS* 1996; 93: 7032–7035.
15. **Verlhac MH, Kubiak JZ, Weber M, Geraud G, Colledge WH, Evans MJ, Maro B**. Mos is required for MAP kinase activation and is involved in microtubule organization during meiotic maturation in the mouse. *Development* 1996; 122: 815–822.
16. **Tong C, Fan HY, Chen DY, Song XF, Schatten H, Sun QY**. Effects of MEK inhibitor U0126 on meiotic progression in mouse oocytes: microtuble organization, asymmetric division and metaphase II arrest. *Cell Res* 2003; 13: 375–383.
17. **Verlhac MH, de Pennart H, Maro B, Cobb MH, Clarke HJ**. MAP kinase becomes stably activated at metaphase and is associated with microtubule-organizing centers during meiotic maturation of mouse oocytes. *Dev Biol* 1993; 158: 330–340.
18. **Lu Q, Dunn RL, Angeles R, Smith GD**. Regulation of spindle formation by active mitogen-activated protein kinase and protein phosphatase 2A during mouse oocyte meiosis. *Biol Reprod* 2002; 66: 29–37.
19. **Yu LZ, Xiong B, Gao WX, Wang CM, Zhong ZS, Huo LJ, Wang Q, Hou Y, Liu K, Liu XJ, Schatten H, Chen DY, Sun QY**. MEK1/2 regulates microtubule organization, spindle pole tethering and asymmetric division during mouse oocyte meiotic maturation. *Cell Cycle* 2007; 6: 330–338.
20. **Xiong B, Yu LZ, Wang Q, Ai JS, Yin S, Liu JH, OuYang YC, Hou Y, Chen DY, Zou H, Sun QY**. Regulation of intracellular MEK1/2 translocation in mouse oocytes: cytoplasmic dynein/dynactin-mediated poleward transport and cyclin B degradation-dependent release from spindle poles. *Cell Cycle* 2007; 6: 1521–1527.
21. **Terret ME, Lefebvre C, Djiane A, Rassinier P, Moreau J, Maro B, Verlhac MH**. DOC1R: a MAP kinase substrate that control microtubule organization of metaphase II mouse oocytes. *Development* 2003; 130: 5169–5177.
22. **Moos J, Visconti PE, Moore GD, Schultz RM, Kopf GS**. Potential role of mitogen-activated protein kinase in pronuclear envelope assembly and disassembly following fertilization of mouse eggs. *Biol Reprod* 1995; 53: 692–699.
23. **Verlhac MH, Kubiak JZ, Clarke HJ, Maro B**. Microtubule and chromatin behavior follow MAP kinase activity but not MPF activity during meiosis in mouse oocytes. *Development* 1994; 120: 1017–1025.
24. **Lefebvre C, Terret ME, Djiane A, Rassinier P, Maro B, Verlhac MH**. Meiotic spindle stability depends on MAPK-interacting and spindle-stabilizing protein (MISS), a new MAPK substrate. *J Cell Biol* 2002; 157: 603–613.
25. **Phillips KP, Petrunewich MAF, Collins JL, Booth RA, Liu XJ, Baltz JM**. Inhibition of MEK or cdc2 kinase parthenogenetically activates mouse eggs and yields the same phenotypes as *mos*$^{-/-}$ parthenogenotes. *Dev Biol* 2002; 247: 210–223.
26. **Lawitts JA, Biggers JD**. Culture of preimplantation embryos. *Methods Enzymol* 1993; 225: 153–164.
27. **Liu L, Oldenbourg R, Trimarchi JR, Keefe DL**. A reliable, noninvasive technique for spindle imaging and enucleation of mammalian oocytes. *Nat Biotechnol* 2000; 18: 223–225.
28. **Hogan B, Beddington R, Constantini F, Lacy E**. Manipulating the Mouse Embryo: A Laboratory Manual, 2 ed. Plainview, NY: Cold Spring Harbor Press; 1994.
29. **Phillips KP, Petrunewich MAF, Collins JL, Baltz JM**. The intracellular pH-regulatory HCO_3^-/Cl^- exchanger in the mouse oocyte is inactivated during first meiotic metaphase and reactivated after egg activation via the MAP kinase pathway. *Mol Biol Cell* 2002; 13: 3800–3810.
30. **Kolajova M, Hammer MA, Collins JL, Baltz JM**. Developmentally regulated cell cycle dependence of swelling-activated anion channel activity in the mouse embryo. *Development* 2001; 128: 3427–3434.
31. **Moos J, Kopf GS, Schultz RM**. Cycloheximide-induced activation of mouse eggs: effects on cdc2/cyclin B and MAP kinase activities. *J Cell Sci* 1996; 109 (Pt 4): 739–748.
32. **Carabatsos MJ, Combelles CM, Messinger SM, Albertini DF**. Sorting and reorganization of centrosomes during oocyte maturation in the mouse. *Microsc Res Tech* 2000; 49: 435–444.
33. **Navarro PA, Liu L, Trimarchi JR, Ferriani RA, Keefe DL**. Noninvasive imaging of spindle dynamics during mammalian oocyte activation. *Fertil Steril* 2005; 83 (Suppl 1): 1197–1205.
34. **Favata MF, Horiuchi KY, Manos EJ, Daulerio AJ, Stradley DA, Feeser WS, Van Dyk DE, Pitts WJ, Earl RA, Hobbs F, Copeland RA, Magolda RL, Scherle PA, Trzaskos JM**. Identification of a novel inhibitor of mitogen-activated protein kinase kinase. *J Biol Chem* 1998; 273: 18623–18632.
35. **Deng M, Williams CJ, Schultz RM**. Role of MAP kinase and myosin light chain kinase in chromosome-induced development of mouse egg polarity. *Dev Biol* 2005; 278: 358–366.
36. **Deng M, Suraneni P, Schultz RM, Li R**. The Ran GTPase mediates chromatin signaling to control cortical polarity during polar body extrusion in mouse oocytes. *Dev Cell* 2007; 12: 301–308.